JOINT INVERSION OF MULTIPLE SEISMIC DATA FOR THREE-DIMENSIONAL VELOCITY STRUCTURE BENEATH SOUTHERN AND EASTERN ASIA

Suzan van der Lee[1], Sung Joon Chang[2], Michael Witek[1], Tae Seob Kang[3], Mei Feng[4]

Northwestern University[1], University of East Anglia[2], Pukyong National University[3], and Chinese Academy of Geological Sciences[4]

Sponsored by the Air Force Research Laboratory

Award No FA9453-11-C-0231

The 3D *S*-velocity structure for the crust and mantle along the Tethyan margin has been modeled through the joint inversion of multiple seismic data such as teleseismic *S*-arrival times, regional waveform fits, fundamental-mode group velocities, and independent Moho constraints (Chang et al., 2010). We now aim to construct a 3-D *S*-velocity model for the crust and mantle beneath eastern Asia using the same joint inversion method, augmented with ambient seismic noise data, gravity data, and converted body wave data. We aim to model the 3D crust and mantle *P*-velocity structure using a scaled version of the 3D *S*-velocity model as a reference model relative to which we invert teleseismic and regional *P* delay times.

Our 3-D *P*-velocity model derived this way for the Tethyan margin (EAPV11) is more uniformly resolved with better depth resolution, including velocity anomalies for aseismic regions with few stations, than is typically obtained from traditional teleseismic delay time inversions. EAPV11 is also able to predict delay times for ground truth (GT25) events, which were not used in the inversion. This implies that although scaling *S* velocities to *P* velocities may be uncertain, the scaled velocities contribute to the accurate prediction of delay times at regional distances. Our planned *S* and *P* velocity models for eastern Asia will be validated using the methods of Flanagan et al. (2007) for regional delay time prediction and Komatitsch et al. (2002) for regional *S* and Rayleigh wave train prediction.

OBJECTIVES

Our primary objective is to construct a high-resolution 3-D model for the *S*-velocity of the mantle and beneath eastern Asia. The model is to have

1) high-resolution crustal structure of Korean peninsula, constrained by gravity data and ambient seismic noise data,

2) consistently good resolution from the surface to the lower mantle obtained from multiple data sets with different resolving powers,

3) topography of seismic discontinuities such as the Moho, which is essential for travel time prediction and seismic phase discrimination, and

4) uncertainties for each data set taken into account to weight individual data sets in the joint inversion according to data quality.

RESEARCH ACCOMPLISHED

We finalized a manuscript on the *P* velocity structure, and its validation, of the mantle along the Tethys Belt (Chang et al., 2012). The *P* velocity model (Fig. 1) is the result of inverting teleseismic *P* arrival times relative to a reference model that was converted to *P* velocity from an *S* velocity model, derived from the joint inversion of teleseismic *S*-arrival times, regional waveform fits, fundamental-mode group velocities, and independent Moho constraints (Chang et al., 2010).

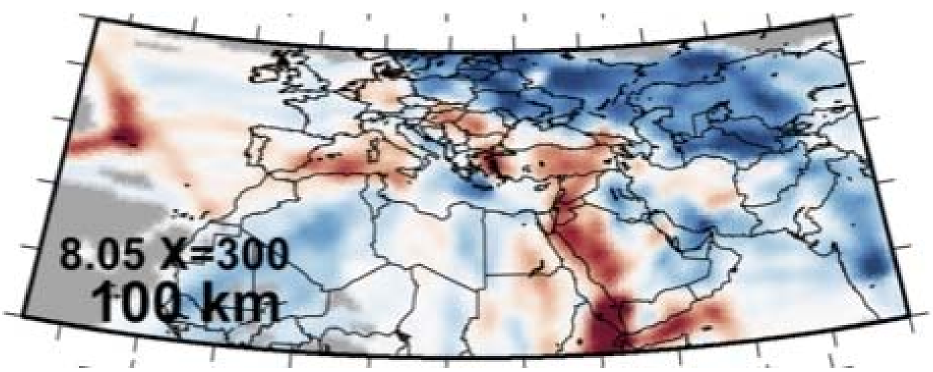

Figure 1. *P* velocity structure at a depth of 100 km beneath the western Tethys Belt. In this project we aim to expand this imaging eastwards to east Asia.

In this project we aim to model the *P* velocity of east Asia similarly, and with enhanced resolution for the crustal structures. A major first step in this process is to model the *S* velocity of east Asia, using the same types of *S* data as in Chang et al. (2010), enhanced with constraints from the dispersion of ambient noise and relative to a three-dimensional starting model in those regions where data access is problematic.

A rough version of the larger study region is provided in Fig. 2. Feng et al.'s (2010) *S* velocity model for this region is based on data from 283 permanent and temporary broadband stations deployed in and around China before 2006. The permanent networks include New China Digital Seismograph Network, the Broadband Array in Taiwan, GEOSCOPE, Global Seismographic Network, and the Kazakhstan Network, among others. The temporary networks/arrays include experiments deployed upon the Tibetan Plateau, in North China, and in NE China, among others. Not all of the Chinese data utilized are publicly accessible. Therefore, we will use this *S* velocity model as a starting model in our inversion. This starting model shows reasonable detail in the crust, owing to the inclusion of group velocity dispersion curves, and significant, resolved heterogeneity in the mantle (Fig. 3). Feng et al. (2010) converted this seismic velocity model to mantle temperatures to study the strength and thickness of the Chinese lithosphere. The velocity structure of Figure 3 also shows that the lithosphere of the North China Craton thins eastwardly, but the Yangtze Craton, Tibetan Plateau, and Tarim Basin, show stronger and thicker lithosphere (see Feng et al., 2010). Also beyond China, the mantle wedge beneath Japan is distinct from other structures in the model.

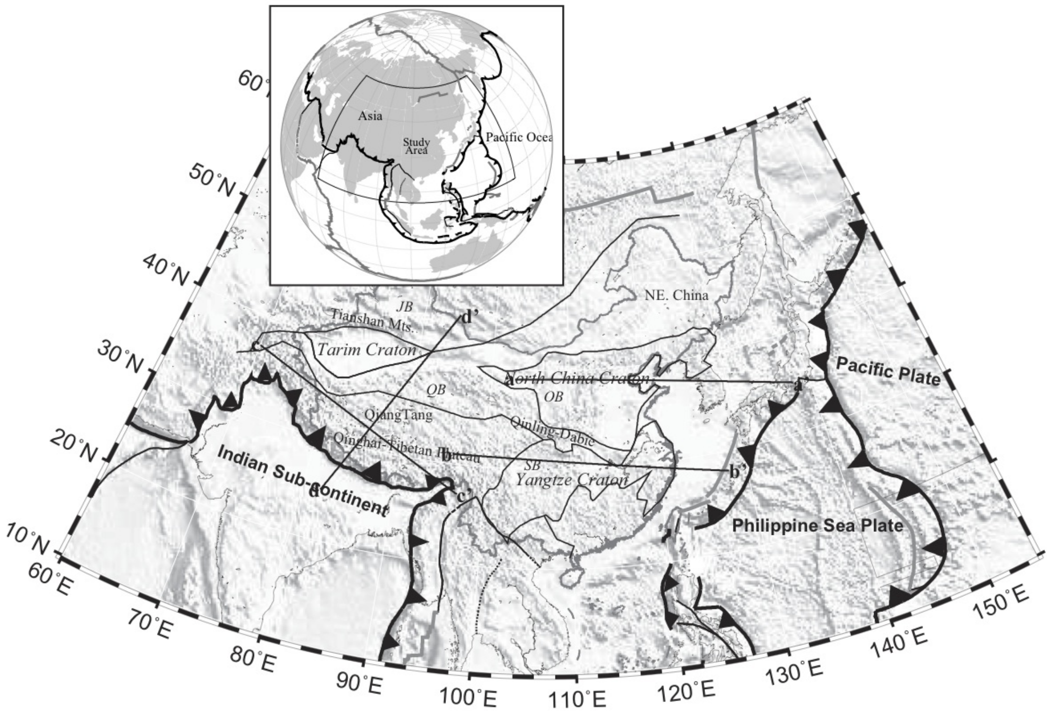

Figure 2. Map of larger study region (from Feng et al. (2010)). Profile aa' (Fig. 3) runs through the North China Craton, the Korean peninsula, and ends near the triple junction of the Eurasian, Pacific, and Philippine Sea plates.

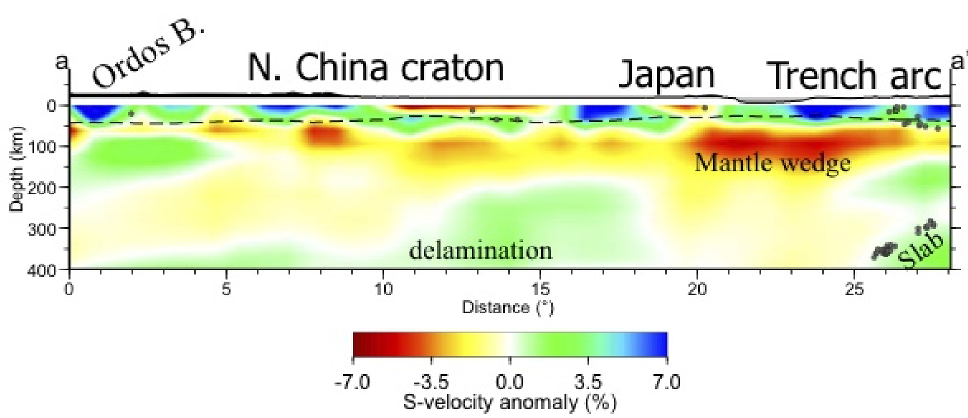

Figure 3. Cross section through the *S* velocity model of Feng et al. (2010) along line aa' of Figure 2. This model shows an eastwards thinning lithosphere beneath the North China Craton and a distinct mantle wedge east of Korean Peninsula (beneath the "n" of the "Japan" label).

Data that will be inverted relative to this starting model will be collected from the stations and events illustrated in Figure 4. The types of data we will collect and analyze are teleseismic *S*-arrival times, regional waveform fits, fundamental-mode group velocities, independent Moho constraints (from receiver function studies, for example Chang and Baag (2007)), and ambient noise dispersion.

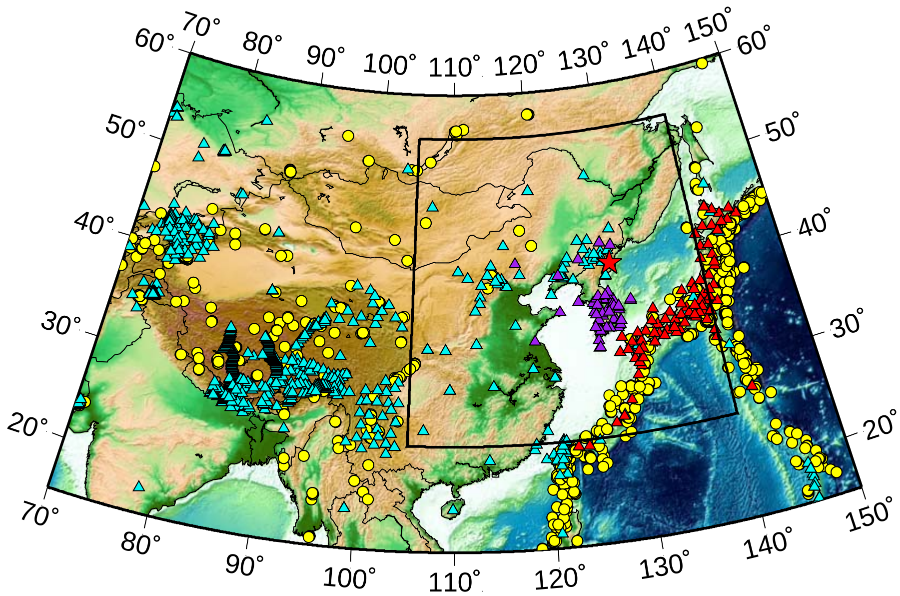

Figure 4. Map of stations which are available for this study and event distribution. Stations from IRIS, Korea, and Japan are indicated by cyan, purple, and red triangles, respectively. Events with magnitude more than or equal to Ms 5.0 from 1998 to 2010 (< 70 km depth) are represented as yellow circles.

We are currently collecting data from F-net (Japan), KIGAM, and KMA (Korea) and preparing to estimate ambient noise dispersion in these data for periods of 5 s and more. These data are essential for improving the resolution of crustal structure in eastern Asia. Inclusion of data from open stations in northeastern China will further optimize regional and azimuthal coverage, including for regions in the Korean Peninsula without accessible data (Figure 5).

The only data type in our collection that is sensitive to lower-mantle structure are the teleseismic arrival times. Resolution of the lower mantle can, however, be improved by consistently better resolving structure of the upper mantle (Chang et al, 2010), because of their shared sensitivity for upper mantle structure. By including dispersion estimates from ambient noise, we anticipate to further improve resolution, from the crust to the lower mantle.

We do not invert solely for *S* velocity anomalies, but also for lateral variations in depths of important seismic discontinuities, specifically the Moho and the 410 and 660-km discontinuities. Having accurate estimates for the depths and lateral variations therein, is essential for travel time predictions and seismic phase discrimination. Ultimately, we will solve the following system of equations in the joint inversion for an *S* velocity model:

$$
\begin{bmatrix}
w_{ta}A_S^{ta} & w_{ta}A_m^{ta} & 0 & 0 & w_{ta}A_{ta,e} & w_{ta}A_{ta,o} \\
w_{rw}A_S^{rw} & w_{rw}A_m^{rw} & 0 & 0 & 0 & 0 \\
w_U A_S^U & w_U A_m^U & 0 & 0 & 0 & 0 \\
0 & w_{ic}A_m^{ic} & 0 & 0 & 0 & 0 \\
w_G A_S^G & w_G A_m^G & 0 & 0 & 0 & 0 \\
w_{410}A_S^{P410s} & 0 & w_{410}A_{410}^{P410s} & 0 & 0 & 0 \\
w_{660}A_S^{P660s} & 0 & 0 & w_{660}A_{660}^{P660s} & 0 & 0 \\
w_1 I & w_1 I & 0 & 0 & 0 & 0 \\
w_2 F_h & w_2 F_h & 0 & 0 & 0 & 0 \\
w_3 F_v & 0 & 0 & 0 & 0 & 0
\end{bmatrix}
\begin{bmatrix}
\Delta V_S \\ \Delta d_{moho} \\ \Delta d_{410} \\ \Delta d_{660} \\ \Delta x_e \\ \Delta e
\end{bmatrix}
=
\begin{bmatrix}
w_{ta}d^{ta} \\ w_{rw}d^{rw} \\ w_U d^U \\ w_{ic}d^{ic} \\ w_G d^G \\ w_{410}d^{P410s} \\ w_{660}d^{P660s} \\ 0 \\ 0 \\ 0
\end{bmatrix}
$$

where A_b^a is a matrix of partial derivatives of a with respect to b. Superscripts *ta, rw, U, ic, G, P410s*, and *P660s* represent teleseismic arrival times, regional waveform fits, Rayleigh-wave group velocities including ambient noise cross-correlation, independent Moho constraints, gravity data, P410s-P and P660s-P phases, respectively. The corresponding data vectors are d^a. Furthermore, ΔV_S, Δd_{moho}, Δd_{410}, Δd_{660}, Δx_e, and Δe are anomalous *S* velocity, depths to Moho, 410, and 660 km discontinuities, event mislocations, and origin time errors, which constitute model parameters. I is the identity matrix for damping operator; F_h and F_v are horizontal and vertical flattening operators, respectively. Weights w are applied to each data set and operator and are used to weight individual data sets according to data quality.

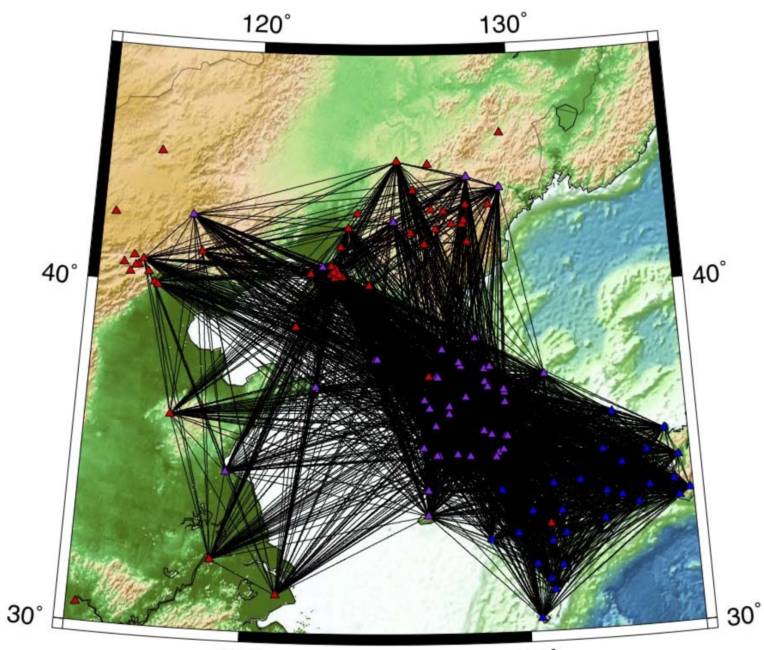

Figure 5. Great-circle paths for ambient noise cross-correlation to measure short-period group velocity data. Stations are the same as in Figure 4.

CONCLUSIONS AND RECOMMENDATIONS

None yet.

REFERENCES

Chang, S.-J., S. van der Lee, M. P. Flanagan, H. Bedle, F. Marone, E. M. Matzel, M. E. Pasyanos, A. J. Rodgers, B. Romanowicz, and C. Schmid (2010). Joint inversion for 3-dimensional S-velocity mantle structure along the Tethyan margin, *J. Geophys. Res.* **115**, B08309, 22 pp., doi:10.1029/2009JB007204.

Chang, S.-J., S. van der Lee, and M. P. Flanagan (2012). A new P-velocity model for the Tethyan margin from a scaled S-velocity model and the inversion of P and PKP delay times, submitted to *PEPI.*

Chang, S.-J. and C.-E. Baag (2007). Moho depth and crustal Vp/Vs variation in southern Korea from teleseismic receiver functions: Implication for tectonic affinity between the Korean Peninsula and China, *Bull. Seismol. Soc. Am*. **97**, 1621–1631.

Feng, M., S. van der Lee, M. An, and Y. Zhao (2010). Lithospheric thickness, thinning, subduction, and interaction with the asthenosphere beneath China from the joint inversion of seismic S-wave train fits and Rayleigh-wave dispersion curves, *Lithos* **120**, 116–130, doi:10.1016/j.lithos.2009.11.017.